Filtering Depth Measurements in Underwater Vehicles for Improved Seabed Imaging

Are B. Willumsen, Ove Kent Hagen and Per Norvald Boge

Abstract— **Underwater vehicles are commonly used for detailed seabed mapping. To derive a bathymetric map, the depth of the underwater vehicle must be known. The offshore survey industry has often strong requirements on both absolute and relative accuracy.**

Depth is usually deduced from a measurement of absolute pressure. Regardless of the quality of the pressure sensor, the pressure measurement is influenced by environmental factors, such as waves, tide, atmospheric pressure and sea water density profile. In the paper we analyze these factors with respect to their behavior and effect on the measured depth.

An underwater vehicle equipped with an aided inertial navigation (AINS) system has through its accelerometers and Doppler velocity log redundant information on the movement of the underwater vehicle. Using this information, an AINS is well suited to filter out dynamic pressure sensor noise. Linear wave theory is used to model the effects of the waves on the pressure sensor, and it is suggested how the parameters of the pressure sensor noise model can be deduced from the mean wave amplitude and period. AINS performance is often substantially improved by post-processing. The paper will therefore examine the depths outputted from the pressure sensor, from the AINS real-time filter, and from post processing the AINS measurements.

Index Terms—**Kalman Filtering, Imaging, Inertial Navigation, Pressure, Depth, Waves**

I. Introduction

In underwater navigation the main focus has been to establish the vehicle's horizontal position using a variety of different aiding techniques [1]. In many applications the vertical position can be deduced directly from pressure measurements with sufficient accuracy. However, with the new requirements on seabed mapping accuracy, the accuracy of straightforward conversion from pressure to depth is challenged. A stable and accurate depth estimate is required for any high accuracy bathymetric mapping sensor mounted on an underwater vehicle. Otherwise, the resulting bathymetry estimate gets distorted with unwanted ripples.

The introduction of terrain navigation also sets high demands on real-time vertical channel accuracy in certain types of bathymetry [2]. Vehicle depth errors can reduce the ability of the terrain navigation system to correlate bathymetric measurements with pre-stored digital terrain models.

The conversion of pressure measurements to depth estimates has traditionally been solved based on an assumption of hydrostatic pressure in the water column above the vehicle [3]. Since 1984 the UNESCO formula [4], has provided a standard for performing this conversion. However, in shallow water operations the influence of a dynamic pressure component induced by surface waves has been observed. In this paper we suggest that the wave induced pressure oscillations can be modelled as noise on the depth measurements fed into an aided inertial navigation system (AINS). This way one combines the superior INS short term estimates with the stable long term estimates from the hydrostatic conversions, and the dynamic pressure variations can be filtered out. The principle of combining inertial and pressure measurements was used for submarines in [5]. The objective and approach there was quite different from this paper.

A. Vertical datum

Depth (and height) is always referenced to a specific vertical datum. Ocean vehicles and airplanes have traditionally been using the mean sea level (MSL). This is the level of the sea at a particular horizontal position, when the effects of waves and tides have been averaged out. The WGS-84 is another important vertical datum and is the one used by GPS. It is defined by the surface of the WGS-84 ellipsoid approximation of the earth geoid.

In this article we will rely upon the MSL vertical datum. However the choice of datum is not important to the task, as conversion from one vertical datum to another is usually a straight forward procedure.

II. Total pressure field

Assuming the underwater vehicle is at rest, and there is no sea current, then according to linear theory of fluid dynamics the total pressure $p_{B_{ps}}$ measured by a sensor on the vehicle,

Manuscript received March 29, 2007.

Are B. Willumsen is with Kongsberg Maritime AS, PO Box 111, 3191 Horten, Norway (+4733023912; fax: +4733047619; e-mail: are.b.willumsen@kongsberg.com).

Ove Kent Hagen is with FFI, PO Box 25, 2027 Kjeller, Norway (e-mail: Ove-Kent.Hagen@ffi.no).

Per Norvald Boge is with Geoconsult AS, Nedre Åstveit 12, 5106 Øvre Ervik Bergen Norway (e-mail: Per.Norvald@geoconsult.no).

TABLE I
A CLASSIFICATION OF OCEAN WAVE TYPES BASED ON THEIR PERIODS,

Period	Wavelength	Type
0-0.2 s	Centimeters	Ripples, capillary waves
0.2-9 s	To about 130 m	Wind waves
9-15 s	Hundreds of meters	Swell
15-30 s	Several hundreds of meters	Long swell, forerunners
0.5 min – hours	To thousands of kilometers	Long period wave, tsunami
12.5, 25 h, …	Thousands of kilometers	Tides

Adopted from [6]

can be described as a superposition of the stationary hydrostatic pressure equilibrium p_h and the dynamic pressure field p_w caused by surface waves

$$p_{B_{ps}} = p_h + p_w . \qquad \text{(II.1)}$$

The incoming waves can be categorized by their period, see Table I. Ripples and capillary waves both have small amplitudes. They decay fast with depth due to viscous forces, and are therefore ignored in this analysis. The incoming wind waves and swell is treated separately from tides in section D. The wave-body interaction is commented on in section E.

A. Tidal wave elevation

Tides act in two natural periods: *semi-diurnal* (about 12.5 hours, common) and *diurnal* (about 25 hours, uncommon). They can in extreme areas be in the order of 7 m amplitude (Bay of Fundy, Canada [6]). In addition, local topography might contribute through to the effect of trapping energy from tides in resonating bays [6]. The local rise and fall of sea level can also be contributed to horizontal variations in atmospheric pressure, and storm surges in costal regions.

On the timescale of wind waves and swells, tides will seem like a stationary process, and the effect of its dynamics is therefore ignored. Hydrostatic pressure to depth conversions will always give an answer relative to current tidal elevation level. To be able to fully utilize depth data, they need to be transformed to the vertical datum.

Tide elevation with respect to MSL at the position of the underwater vehicle should therefore be measured or estimated. It can be measured from a surface ship using a high quality GPS system, or by bottom mounted pressure sensors, or wave gauges at shore. Local tide estimates can also be based on of the official services for tidal predictions, possibly corrected by measured data.

The hydrostatic pressure to depth calculation has its zero level at the tidal level and the estimate of the tide elevation above MSL must be subtracted to yield the depth below MSL.

B. Atmospheric pressure

At the sea surface the boundary condition on the subsurface pressure field implies that it by continuity must equal the sea surface atmospheric pressure p_0. The atmospheric pressure must be subtracted from the absolute pressure measured by the pressure sensor on the underwater vehicle.

If a surface vessel is present, the atmospheric pressure can easily be measured and updates can be sent to the underwater vehicle, if needed. If the vehicle is operating autonomously, the vehicle itself can measure the atmospheric pressure when surfacing, or it can use the best available weather forecast for the operation area. If none of these data are available, the best one can do is to subtract the standard atmospheric pressure of 101325 Pa (1.01325 bar). Assuming that this is an unbiased estimate, the maximum error in doing so is in the order of 0.35 m.

For the case of post-processing, better data can be obtained by including measurements from the nearest weather stations as well. If the weather station is situated above the MSL, the pressure also needs to be compensated for this altitude.

As an approximation we will consider the atmospheric pressure to be measured at the tidal elevation level instead of the actual sea surface level. The error in doing so is less than 0.01 m in most cases [11] .

C. Hydrostatic pressure field

For the hydrostatic pressure field, wave elevation and motion is neglected except for wavelengths in the order of tidal waves. Since the wavelength of the tidal wave is much larger than the horizontal extent of the water column above the vehicle, the pressure field in the water column above the vehicle is assumed to only depend on depth.

The main contributions to change in density with depth are from compressibility of seawater at high pressure *p*, change in *salinity S* with depth, and finally change in temperature *T* with depth.

The specific volume $V(S,T,p)$ is defined as a function of salinity, temperature and pressure based on the equation of state EOS80. In [4] it is shown that the relationship between pressure and depth z under these assumptions is approximated by

$$z = \frac{\int_{p_0}^{p} V(35,0,p)dp}{g_0(\mu)\left(1+\frac{1}{2}\gamma_p(p-p_0)\right)} + \frac{1}{9.8}\int_{p_0}^{p}\delta(p)dp . \qquad \text{(II.2)}$$

Here $g_0(\mu)$ is sea surface gravity at latitude μ, and γ_p is the mean vertical gradient of gravity with respect to pressure in the water column.

The first integral of (II.2) represent the assumption of *standard ocean* (S= 35 psu and T = 0°C). In [4] a 4th order polynomial fit to this integral has been calculated, and this serves as the standard of today.

The integral of the specific volume anomaly δ in (II.2) is the geopotential anomaly, and represents corrections according to the actual density profile of the water column. The integral can be calculated numerically from a CTD profile of the water column The error in ignoring this term can in some areas be substantial (e.g. 2.3% of depth in the Baltic Sea [11]). The integral can also be approximated by geographically dependent equations of the pressure [8].

D. Waves

The dynamic pressure field generated by surface waves can

be analyzed using linear wave theory. For simplicity we restrict the analysis to 2D. Assuming the wave velocity vector field is curl-free, there exists a velocity potential $\phi_w(x,z,t)$. For an incompressible fluid the velocity potential solves Laplace's equation in the fluid volume

$$\nabla^2\phi_w = 0 . \qquad \text{(II.3)}$$

The following boundary conditions are given:

- No normal velocity at bottom depth $z = h$.
- The surface $z = \eta(x,t)$ and the fluid particles have the same vertical velocity at the tidal elevation level.
- Continuity in surface pressure

For a sinusoidal surface wave $\eta(x,t) = a\sin(kx - \omega t)$ with amplitude a, wave number k and angular frequency ω, the solution to the PDE in (II.3) with these boundary conditions is,

$$\phi_w(x,z,t) = \frac{ag}{\omega\cosh(kh)}\cosh(k(h-z))\cos(kx-\omega t) . \qquad \text{(II.4)}$$

Here g denotes the gravitational acceleration, assumed to be constant. The corresponding *dispersion relation* can be found from the boundary conditions at the surface, and is given by

$$\omega^2 = gk\tanh(kh) . \qquad \text{(II.5)}$$

Now, using the linear version of Euler's equations we get the following relationship between the velocity potential field and the pressure field

$$p_w = -\rho\frac{\partial\phi_w}{\partial t} . \qquad \text{(II.6)}$$

Here ρ denotes the seawater density. By inserting (II.4) into (II.6), we obtain the subsurface dynamic pressure field caused by a sinusoidal surface wave,

$$p_w(x,z,t) = -\rho g\frac{\cosh(k(h-z))}{\cosh(kh)}\eta(x,t) . \qquad \text{(II.7)}$$

These equations are all valid for the linear case only. The requirement for linear wave theory to be an adequate model is given by a restriction on wave steepness (ratio of wave amplitude to wavelength) given by $ak \ll 1$, for both the deepwater and shallow water cases. Additionally it is required that the wave amplitudes are much smaller than the water depth, so $a/h \ll 1$ for the shallow water case.

Also the ideal fluid approximation leads to an unphysical condition at the seafloor, where a "no slip" condition is a more realistic condition to apply.

The assumption of uniform bottom depth is in general not good for littoral waters, as the interactions with bathymetry severely influence wave amplitude, period and direction of propagation. The linear model will however provide a first order approximation and insight into the effects there.

1) Ocean wave spectrum

The free surface is now considered as a superposition of sinusoidal waves with random amplitude and phase. In [7] a formal representation of the irregular sea surface is given. It is common to describe the surface statistically by the *ocean wave spectrum* $S_\eta(\omega)$, which is a distribution describing how the wave energy is distributed with respect to wave frequency. In 3D the energy spectrum is typically directional, so the above spectrum is considered as the result by integration over all wave directions.

The characterizing moments of the spectrum are defined by

$$m_i \equiv \int_0^\infty \omega^i S_\eta(\omega)d\omega \quad , i = 0,1,2,\ldots . \qquad \text{(II.8)}$$

From the wave spectrum moments, assuming a Rayleigh distribution of wave amplitudes [7], several characterizing variables may be derived using (II.8), such as

- Average wave height, $\bar{H} = \sqrt{2m_0}$.
- Significant wave height, $H_s = 4\sqrt{m_0}$.
- Average angular frequency, $\bar{\omega} = \sqrt{\frac{m_1}{m_0}}$.

One of the most used spectrums to describe a not fully developed state at sea is given by the JONSWAP spectrum [9].

By using the subsurface pressure field representation (II.7), it is straightforward to derive the spectrum for the surface wave induced pressure oscillations as a function of depth [11] .

$$S_{p,h}(\omega,z) = \left(\rho g\frac{\cosh(k(\omega)(h-z))}{\cosh(k(\omega)h)}\right)^2 S_\eta(\omega) . \qquad \text{(II.9)}$$

Here the wave number is a function of the angular frequency implicitly defined through the dispersion relation (II.5). In numerical calculations, the wave number can be found using Newton's method.

Using hydrostatic conversions for these pressure oscillations, the spectrum of the corresponding depth oscillations $S_h(\omega,z)$ is found from the approximation

$$S_h(\omega,z) = \left(\frac{\cosh(k(\omega)(h-z))}{\cosh(k(\omega)h)}\right)^2 S_\eta(\omega) . \qquad \text{(II.10)}$$

A demonstration of how a JONSWAP spectrum of surface waves attenuates with depth is shown in Fig. 1. It shows that the high frequency waves attenuate faster with depth than the

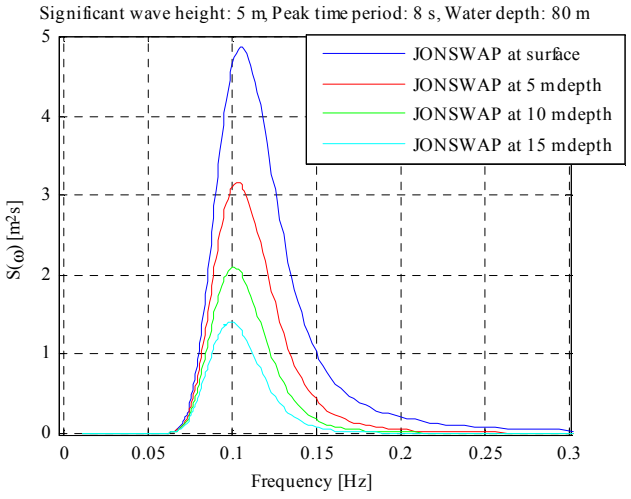

Fig. 1. JONSWAP spectrum at different depths

low frequency waves, so the energy is shifted relatively towards lower frequency with depth.

E. Other aspects

If the pressure transducer is positioned at areas on the hull exposed to stagnation pressure effects, this will inflict an error in the measurement. Also the non-zero velocity of the vehicle with reference to the wave field causes a Doppler shift of the measured pressure waves. The wave-body interaction is also a source of deviation in the measured pressure. All these aspects are closely discussed in [11]. The effects are not important to this analysis and are as such omitted.

III. Filtering with an AINS

The aided inertial navigation system (AINS) integrates accelerations and angular rates from an inertial measurement unit (IMU) into speed, orientation and position. It has low short term errors, but will drift in the long term. It is therefore dependent upon aids to reduce the integrated error. For underwater vehicles, such aids are usually pressure sensor, DVL, LBL and USBL.

A. Static and semi-static errors

For underwater vehicles, there is almost no other measurement that can provide an accurate depth reference. It is therefore usually not possible to calibrate the pressure to depth conversion, nor is it possible to on-line estimate a (semi-) static error in the pressure sensor depth measurement. The correction for atmospheric pressure, tide, and geopotential anomaly must be done to get an unbiased global depth. This could be done both on- and off-line, since this causes the AINS to have a close to constant deviation from the true depth.

B. Dynamic errors

The dynamic errors caused by waves of different sort (see Table I), can though be estimated in the AINS. In essence it means that long term accuracy of the pressure sensor and the short term accuracy of AINS are combined to give an accurate short and long term depth estimate.

In order to get an optimal integration of the pressure sensor into the AINS, one must provide a model of the development of the dynamic depth error of the pressure sensor. One of the simplest and easiest approximations of the error propagation is the first order Gauss-Markov process, which is completely specified by the autocorrelation function:

$$r_1(\tau, z) = \sigma_1^2(z) e^{-|\tau| / T_1(z)}. \qquad \text{(III.1)}$$

The standard deviation σ_1 and the inverse of the correlation time T_1 are as a first suggestion the mean wave amplitude and half average wave period respectively at the vehicle's depth. However closer investigations suggest a lower T_1, in the range 1-3 seconds. In [11] an optimal choice for these parameters is derived for the case of regular sinusoidal waves. At sea one usually does not have as detailed information as a wave spectrum, but as we will see in section IV, the AINS is robust with respect to these parameters. Observations of significant wave height and peak time periods for the waves will probably suffice in a realistic scenario.

IV. Simulations

NavLab a generic navigation tool [10], has been used as the environment for the simulations. In the simulation scenario the INS is aided by pressure sensor, DVL, and USBL. The vehicle is kept stationary at 15 m depth, and the ocean depth is 80 m. The surface waves are assumed sinusoidal, and the corresponding effect on the pressure sensor is calculated using (II.7). The resulting depth estimates of a 2 m surface wave with a period of 9 s are shown in Fig. 2 and the standard deviations from true depth is shown in Table II.

The simulations are performed with a navigation grade IMU, standard type of DVL and high class depth sensor.

Both the effect on the pressure at the depth of the vehicle and the parameters of the surface waves themselves can be hard to measure or estimate. It is therefore important to examine the filtering methods robustness against inaccurate or wrongful parameter estimates. For that reason the filter was tested with parameters that did not match the waves in the simulation. The result is seen in Fig. 3, where a surface wave of 2 m amplitude and 9 s period (corresponding to 0.67 m amplitude and 9 s period at 15 m depth) is simulated. The parameters are set according to a typical configuration of 0.15 m standard deviation and 120 s correlation time. The results show that the real-time solution is sensitive to parameter errors whereas the smoothed solution is not.

TABLE II
Simulated waves and resulting standard deviations

Period [s]	Surface amplitude [m]	Measured [m]	Real-Time [m]	Post-Processed [m]
15	2	1.09	0.09	0.04
12	2	0.94	0.08	0.04
9	2	0.67	0.06	0.03
6	2	0.27	0.04	0.02

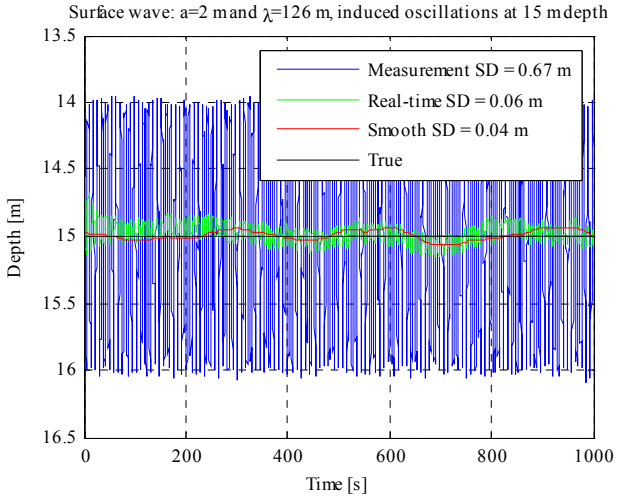

Fig. 2. Simulated depth estimates of waves with period 9s

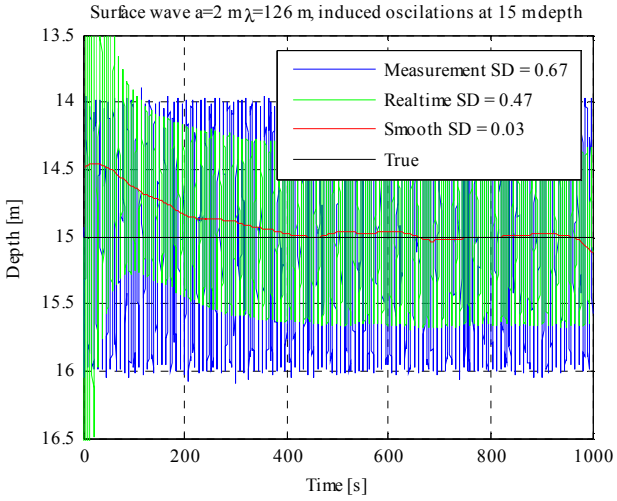

Fig. 3 Simulated depth estimates, with waves (amplitude 2m, period 9s), but AINS parameters corresponding to a typical configuration (0.15m, 120s)

V. Results from collected data

Instead of dedicated sea-trials we will use navigation data from a survey missions performed with ROV. This is a real mission and we have no true reference. Therefore the smoothed solution is what is closest to the truth and will be used as a reference.

The ROV survey was performed from 29th of January 2007 at about 110 meters depth. Fig. 4 shows the mission depth. The deviation from post-processed depth is shown in Fig. 5. It shows that the wave effect is only partially removed from the data with the real-time filtering of the AINS. Fig. 7 is showing DTM generated with the measured depth and with the post-processed depth of Fig. 6 (same time frame). The figure shows a clear ripple effect in the former, whereas in the latter this effect is almost entirely filtered out. Besides showing the improvement in using AINS filtered depth, this supports our claim of using the post-processed depth as a reference.

We also tried using different parameter sets for these data. Although not shown here, the results verified the findings in the simulations. The real-time solution is sensitive to parameter settings whereas the post-processed solution is robust and will generate the same result with different parameters.

VI. Conclusions

This paper has shown that it is advantageous to use AINS in order to obtain a smooth and more correct depth estimate than the one given from a pressure sensor. With the AINS one is able to filter out the effects of pressure fluctuations caused by surface waves. The fluctuations decrease with depth, and so also the benefit of the AINS. Real-time estimates are usually a clear improvement over the measured ones. However simulations and experiments show that these results can often be well improved by the use of post-processing. Both simulations and experimental data show that post processed estimates are smooth, precise, and as opposed to real-time

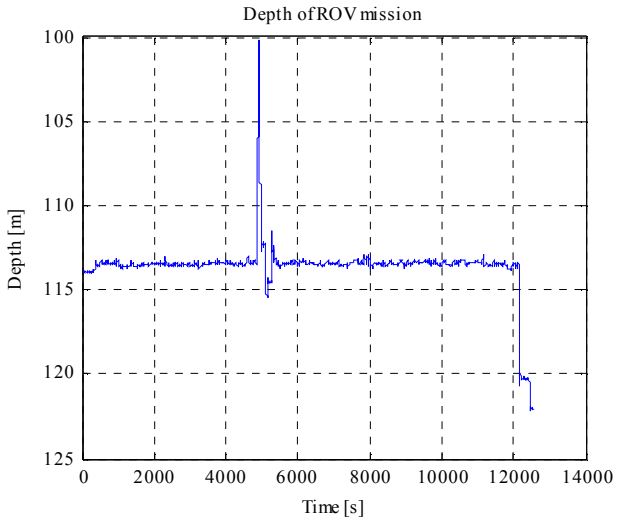

Fig. 4 Depth of ROV trajectory

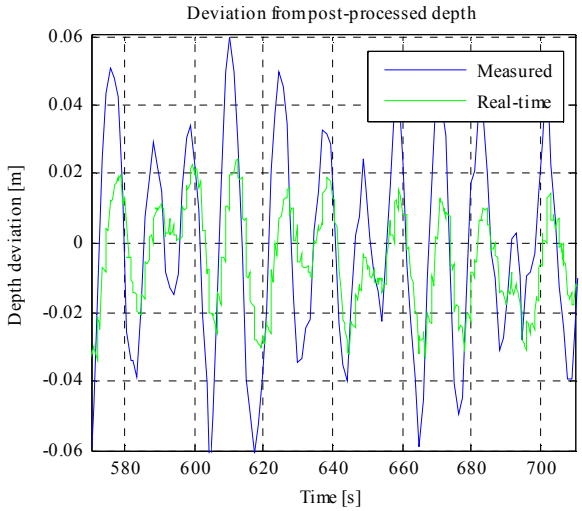

Fig. 5 The deviation of measured and real-time estimated depths from post processed estimate

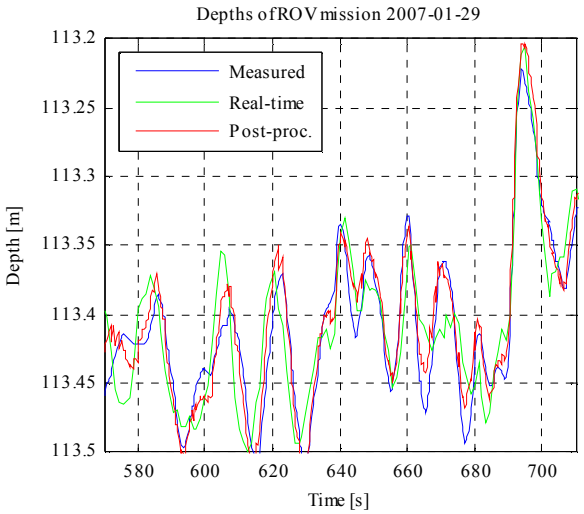

Fig. 6 Measured, real-time and post-process estimated depths of mission 2007-01-29

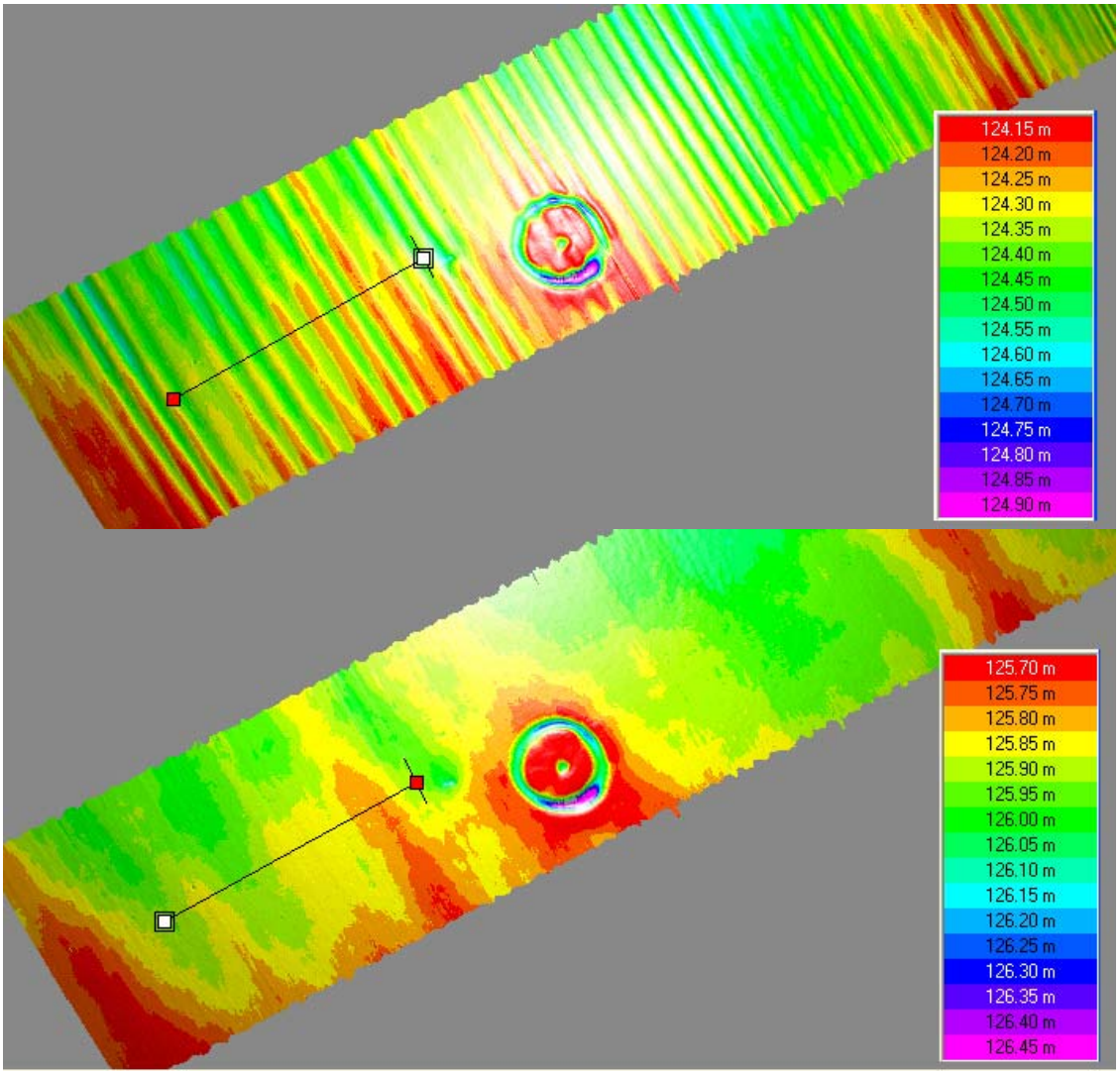

Fig. 7 DTM generated by the use of measured depths (top) and post-processed depths (bottom) shown in Fig. 6

estimates, robust with reference to parameter settings.

Maps generated with AINS and pressure sensor are clearly better than the ones generated with only a pressure sensor. Ripple caused by surface waves are almost eliminated when using post-processed navigation data to generate the map.

REFERENCES

[1] B. Jalving, K. Gade, O. K. Hagen and K. Vestgård, "A Toolbox of Aiding Techniques for the HUGIN AUV Integrated Inertial Navigation System," *Proceedings from OCEANS 2003*,

[2] O. K. Hagen and P. E. Hagen, "Terrain Referenced Integrated Navigation (TRIN)," *BP02 MREA 2003 Conference Proceedings*, NATO Undersea Research Centre, La Spezia, Italy, May

[3] B. Jalving, "Depth Accuracy in Seabed Mapping with Underwater Vehicles," *Proceedings from Oceans 99*, Seattle, WA, USA

[4] N. P. Fofonoff and R. C. Millard Jr., "Algorithms for computation of fundamental properties of seawater," *Unesco technical papers in marine science 44*, 1983

[5] M. Glass and J. A. M. ter Horst, "Combining pressure and Inertial Measurements For Submarine Depth Determination," *Naval Engineers Journal*, vol 98, no. 6, pp 62-68, 1986

[6] S. Pond, G. L. Pickard, *Introductory Dynamical Oceanography*, Oxford, UK: Pergamon Press, 1983.

[7] J. N. Newman, *Marine Hydrodynamics*, The MIT Press, Cambridge, Massachusetts 1977.

[8] C. C. Leroy and F. Parthiot, "Depth-pressure relationships in the oceans and seas," *Journal of the Acoustical Society of America*, vol 103, no. 3, pp 1346-1352, March 1998

[9] K. Hasselmann, T. P. Barnett, E. Bouws, H. Carlson, D. E. Cartwright, K. Enke, J. A. Ewing, H. Gienapp, D. E. Hasselmann, P. Kruseman, A. Meerburg, P. Møller, D. J. Olbers, K. Richter, W. Sell, and H. Walden, "Measurements of wind-wave growth and swell decay during the Joint North Sea Wave Project (JONSWAP)," *Ergnzungsheft zur Deutschen Hydrographischen Zeitschrift Reihe* A(8) (Nr. 12): 95.

[10] K. Gade, "NavLab, a Generic Simulation and Post-processing Tool for Navigation," *European Journal of Navigation,* vol 2, no. 4, pp. 51-59, 1994.

[11] O. K. Hagen and B. Jalving, "Converting Pressure to Depth for Underwater Vehicles", Norwegian Defence Research Establishment (FFI), Tech. Report., unpublished